JOURNAL OF SOLID STATE CHEMISTRY 119, 176–190 (1995)

Acid-Leaching of Sodium Brannerite: Synthesis and Structure of $Na_{0.13}(V_{0.13}Mo_{0.87})O_3 \cdot nH_2O$

Yatao Hu and Peter K. Davies[1]

Department of Materials Science and Engineering, University of Pennsylvania, Philadelphia, Pennsylvania 19104-6272

Received January 17, 1995; in revised form May 16, 1995; accepted May 17, 1995

In dilute hydrochloric acid $NaVMoO_6$, which has a layered "brannerite" structure, participates in an acid-leaching reaction that results in the formation of a metastable compound with the stoichiometry $Na_{0.13}(V_{0.13}Mo_{0.87})O_3 \cdot nH_2O$ and the structure of "hexagonal" MoO_3. The locations of the sodium ions and water molecules in the channels of this structure, space group $P6_3$ with $a = 10.628(1)$ Å and $c = 3.6975(7)$ Å, were determined through Rietveld refinement of powder neutron diffraction data collected on deuterated samples. The water molcules are important in providing a stable environment for the sodium ions, which are octahedrally coordinated by four framework oxygen atoms and two water molecules. In an attempt to understand the mechanistic aspects of the acid-leaching reaction, samples of the hexagonal phase were formed with a range of V : Mo contents from aqueous Na–V–Mo solutions via conventional precipitation methods. Although phases could be stabilized with the same crystallography as the brannerite-derived products, the solution precipitates contained vacancies in the transition metal framework and a higher concentration of sodium in the channels. These compositional differences led to a significant reduction in the apparent high-temperature stability of the solution-derived phases compared to that of their brannerite-derived counterparts. There is some evidence to suggest that the structural filiation between brannerite and hexagonal MoO_3 may be responsible for the unique stoichiometry and stability of the products of the acid-leaching reactions and that the acid-leaching reactions do not proceed through a simple dissolution/precipitation mechanism. © 1995 Academic Press, Inc.

1. INTRODUCTION

In a series of recent papers (1–4) we have reported on the soft chemical synthesis of new oxides with the hexagonal MoO_3 structure via the acid-leaching reactions of alkali brannerites and by direct precipitation from Li–V–Mo aqueous solutions. In particular we found that complete dehydration of the protonic form of vanadium-stabilized hexagonal MoO_3, $H_{0.13}(V_{0.13}Mo_{0.87})O_3 \cdot nH_2O$, yielded the open form of hexagonal MoO_3, a structure that contains empty one-dimensional channels with free diameters approaching 3.3 Å. The original observations of the unusual leaching reactions of the brannerites were made during investigations of the Na isomorph $NaVMoO_6$ (1). In contrast to the ion-exchange reactions commonly encountered for many layered covalent oxides, when sodium brannerite is immersed in dilute mineral acid the vanadium ions are preferentially leached from the oxide layers, leaving a molybdenum-rich product with a Mo : V content of 6.7 : 1. This reaction proceeds through a two-phase mixture of the starting structure and the final product, $Na_{0.13}(V_{0.13}Mo_{0.87})O_3 \cdot nH_2O$, which was shown to have the hexagonal MoO_3 structure. In this paper the acid-leaching reactions of $NaVMoO_6$ are reexamined to investigate if they represent a unique route to the formation of $Na_{0.13}(V_{0.13}Mo_{0.87})O_3 \cdot nH_2O$. These studies involved characterization of the structures and thermal stabilities of the sodium form of hexagonal MoO_3 prepared from brannerite and by traditional precipitation techniques.

The compounds $A_x(V_xMo_{2-x})O_6$ ($x = 1$, A = Li or Na; $x = 0.8$, A = K) (5) adopt the layered structure of the mineral brannerite ATi_2O_6 (A = U, Th) (6). This structure contains infinite zigzag sheets of edge-sharing MO_6 (M = V, Mo) octahedra separated by alkali ions, which in the case of sodium occupy an octahedral interlayer position (see Fig. 1a). Due to the strong intralayer covalent bonding and weak interlayer electrostatic bonding, it might be expected that the brannerites would undergo rapid proton exchange reactions in dilute acids. Although potassium brannerite does undergo a partial ion-exchange reaction (7), the lithium and sodium isomorphs participate in a partial solvolysis reaction in which the preferential leaching of vanadium from the framework leads to the formation of new compounds with the stoichiometry $A'_{0.13}(V_{0.13}Mo_{0.87})O_3 \cdot nH_2O$ (A' = H, Na) and the structure of hexagonal MoO_3 (see Fig. 1b) (1–3).

Two families of compounds with the hexagonal MoO_3 structure have been reported in the literature. The hexagonal molybdates $AMo_{6-x}(\phi_{Mo})_xH_{6x-1}O_{18}$ have been prepared with $x \approx 2/3$ for A = Na · $2H_2O$, Ag · $2H_2O$, K, Rb, Cs, and NH_4 (8) and $x = 1$ for A = K and NH_4

[1] To whom correspondence should be addressed.

0022-4596/95 $12.00

(9,10) by precipitation from acidified aqueous molybdate solutions (ø represents a vacancy). In this family of compounds the structure is stabilized through the incorporation of the larger monovalent cations in the one-dimensional channels which are charge-compensated by molybdenum vacancies in the framework. Recently it was shown that repeated ion exchange of the hexagonal sodium molybdate in 6 *N* HNO_3 produces a hexagonal hydrate, $MoO_3 \cdot 0.55H_2O$, which can be dehydrated to an open hexagonal form of MoO_3 in which the channels of the structure are unoccupied (11). The second group of compounds, vanadium-stabilized hexagonal molybdates $A_x(V_xMo_{1-x})O_3$ with $0.11 \leq x \leq 0.14$, can be prepared by traditional solid-state methods for A = K, Rb, Cs, and NH_4 (12, 13) and via the acid-leaching reaction of brannerite for $A = H \cdot nH_2O$, $Li \cdot nH_2O$, and $Na \cdot nH_2O$ (1, 2, 3). In this case the channel cations are charge-balanced through the partial substitution of vanadium into the molybdate framework. We have shown that $(Li_xH_{1-x})_{0.13}(V_{0.13}Mo_{0.87})O_3 \cdot nH_2O$ can also be prepared by direct precipitation from acidified Li–V–Mo aqueous solutions within a very narrow range of solution composition and pH (4). The ion-exchange reactions of the lithium-containing compounds can be used to synthesize $H_{0.13}(V_{0.13}Mo_{0.87})O_3 \cdot nH_2O$, which on heating to 350°C yields the open form of vanadium-stabilized hexagonal MoO_3, $(V_{0.13}Mo_{0.87})O_{2.935}$.

This paper focuses on the preparation and properties of vanadium-stabilized, hexagonal sodium molybdates synthesized via the leaching reaction of $NaVMoO_6$ and through direct precipitation from acidified Na–V–Mo aqueous solutions. Although the products of the precipitation reactions are closely related to those obtained from the partial solvolysis reactions of sodium brannerite, the brannerite-derived compounds were found to exhibit a unique stoichiometry and enhanced thermal stability compared to their solution-derived counterparts.

2. EXPERIMENTAL

$NaVMoO_6$ was prepared by solid-state reaction between $NaVO_3$ and α-MoO_3 using the approach reported by Galy and Darriet (5). For the leaching reactions 10.0 g of $NaVMoO_6$ was stirred in 500 ml of 0.25 *M* HCl (aq) for 18 hr at 60°C, and the residual solids were collected by vacuum filtration and dried in a desiccator. The process was repeated, usually once or twice, until all of the starting brannerite structure had been transformed.

For the precipitation reactions mixtures of V_2O_5 and α-MoO_3 with a total transition metal (V + Mo) concentration of 0.05 mol were dissolved in 150 ml 1.0 *M* NaOH(aq). The pH of these solutions was lowered to 1.0 through the addition of the requisite amount of 1.0 *M* HCl(aq); the acidification was monitored using an Orion SA720 pH meter. No attempt was made to further control the pH of the solution, which was heated and stirred at 80°C for 2 hr. The resultant precipitates were collected by vacuum filtration and dried in a desiccator.

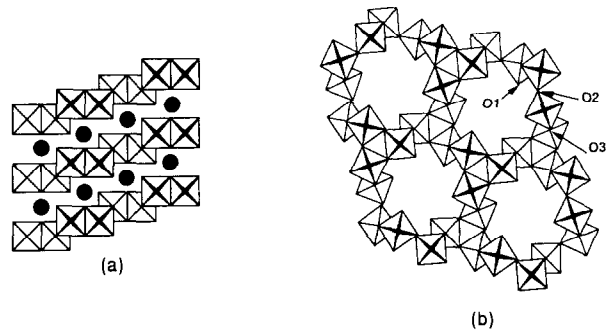

FIG. 1. Idealized projections of (a) $NaVMoO_6$ along [010] and (b) hexagonal MoO_3 along [001].

Phase identification of the reaction products was accomplished using powder X-ray diffraction (Rigaku DMAX-B diffractometer and Cu$K\alpha$ radiation). The morphology of the products was examined using scanning electron microscopy (SEM); chemical compositions were analyzed by atomic absorption (AA) and thermogravimetric analyses (TGA), and a SETARAM DSC111 was utilized to study the thermal stabilities.

Powder neutron diffraction was used to refine the structure of $Na_{0.13}(V_{0.13}Mo_{0.87})O_3 \cdot nH_2O$ by the Rietveld method. The neutron data were collected on deuterated samples prepared by exchanging $Na_{0.13}(V_{0.13}Mo_{0.87})O_3 \cdot nH_2O$ in D_2O at 60°C under a dry nitrogen atmosphere; the samples were sealed in an aluminum container. The diffraction data were obtained using the triple-axis spectrometer on the H4S beamline at the high flux beam reactor (HFBR) at Brookhaven National Laboratory. A Si (400) incident beam monochromator provided a neutron beam with a wavelength of 1.358 Å; the data were collected at room temperature from 10 to 120° in 0.1° steps.

3. RESULTS AND DISCUSSION

3.1. The "Leaching Reaction" of $NaVMoO_6$

To observe the evolution of the leaching of $NaVMoO_6$ in 0.25 *M* HCl at 60°C, the solids present in the solution were collected and examined by X-ray diffraction at different stages of the reaction. The powder pattern of sodium brannerite prior to reaction is shown in Fig. 2a and can be indexed using the cell reported by Galy and Darriet (5) with a = 9.422 Å, b = 3.656 Å, c = 7.228 Å, and β = 111°. The second pattern, Fig. 2b, was obtained from powders that had been reacted for 16 hr in 0.25 *M* HCl. This pattern contains peaks from residual amounts of sodium brannerite and an additional set of reflections that

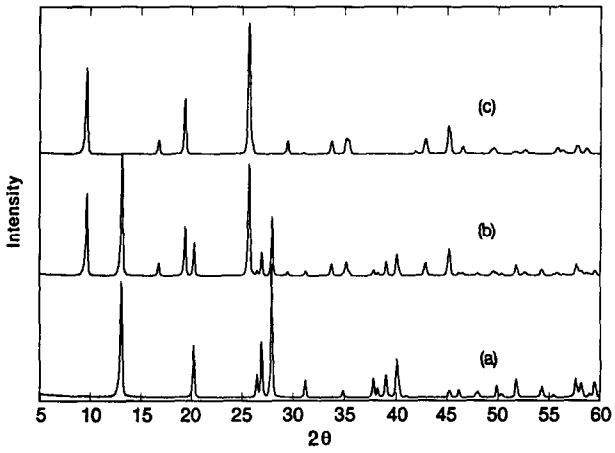

FIG. 2. X-ray diffraction patterns illustrating the evolution of the acid-leaching of $NaVMoO_6$: (a) before treatment; (b) after 16 hr in 0.25 *M* HCl; (c) after 48 hr of reaction.

can be indexed using a hexagonal unit cell. The absence of any shift in the positions of the brannerite peaks confirms the lack of any ion-exchange reaction, though it should be noted that some of the relative intensities are different from those observed in Fig. 2a. The third pattern that appears in Fig. 2c was collected from powders that had been subjected to two additional 16-hr acid treatments. This pattern now contains only a single set of reflections from the hexagonal phase that could be fitted to a cell with $a = 10.628(2)$ Å and $c = 3.696(1)$ Å. This cell is in good agreement with that expected for the "hexagonal MoO_3-type" structure shown in Fig. 1b. The powder patterns of other samples collected at different stages of the reaction confirmed that the conversion of sodium brannerite to the hexagonal phase proceeds through a two-phase mixture of the starting compound and the final product.

The growth of the hexagonal phase at the expense of brannerite is further illustrated by the SEMs in Fig. 3. The image in Fig. 3a was obtained from the starting samples of sodium brannerite; the particles are granular in shape with sizes ranging from 2 to 10 μm. After the first 16-hr acid treatment faceted particles with a well-defined hexagonal prismatic form are clearly visible among the solid products; see Fig. 3b. It is possible to identify thin platelets of the residual brannerite phase at the bottom of this micrograph. The change in the morphology of the brannerite particles presumably results from a preferential solvolysis along the [010] direction, which is perpendicular to the zigzag brannerite layers, and is responsible for the change in the relative intensities of the Bragg reflections from the structure that was noted above. The micrograph in Fig. 3c was collected after a second acid treatment and contains only a few remaining grains of brannerite. A final acid treatment yields a single-phase hexagonal product as is evident from the morphologies of the grains in Fig. 3d; the lengths of the hexagonal prisms range from 5 to 15 μm.

The metal concentrations in the hexagonal phase were determined by AA analyses and corresponded to a composition $Na_{0.13}(V_{0.13}Mo_{0.87})O_3 \cdot nH_2O$; although small variations in the degree of hydration were found from sample to sample, thermogravimetric analyses gave an average value of $n \approx 0.26$. The large reduction in the concentration of vanadium in the solid phases during the reaction is consistent with the expected relative solubilities of V and Mo under these acidic conditions, though it is not clear that the path of the reaction can be described by a simple dissolution–precipitation mechanism.

The dehydration and rehydration of $Na_{0.13}(V_{0.13}Mo_{0.87})O_3 \cdot nH_2O$ were studied by TGA under an argon gas flow; see Fig. 4. The dehydration reaction starts at temperatures as low as 30°C and is complete at about 300°C; the total weight loss corresponds to approximately 0.26 mole of H_2O per formula unit. Because the loss of water is gradual and shows no significant discrete steps, it is difficult to distinguish between water molecules that may have different bonding environments. However, the results of a structure refinement (see Section 3.3) indicate that only about one-third of the total weight loss is due to water contained within the structure, implying that the remaining two-thirds are adsorbed on the surface of the hexagonal crystallites as H_2O or –OH groups.

Although $Na_{0.13}(V_{0.13}Mo_{0.87})O_3 \cdot nH_2O$ can be fully dehydrated at 300°C without bulk decomposition, the dehydrated form readily rehydrates upon cooling even under a nominally dry argon atmosphere; see Fig. 4. This behavior is consistent with the results of the structure refinements where the presence of the water molecules in the channels was found to be essential for the completion of the coordination environment of the Na ions. The water content of the rehydrated samples is consistently lower than that in the starting materials; under a water-saturated argon atmosphere slowly cooled samples only recovered approximately 0.09 mole of H_2O per formula unit. The water that is recovered upon cooling appears to enter the structure, and the lattice parameters of the rehydrated samples are identical to those of the starting samples. The degree of rehydration is also in close agreement with the composition of the starting material obtained from neutron refinement and supports a formula $Na_{0.13}(V_{0.13}Mo_{0.87})O_3 \cdot 0.09H_2O$.

The thermal stability of $Na_{0.13}(V_{0.13}Mo_{0.87})O_3 \cdot nH_2O$ was examined by DSC; aside from a small exothermic peak at 500°C no discrete transitions were observed. The 500°C transition was found to be higher than the bulk decomposition temperature of the hexagonal structure, which was examined by annealing samples at a series of temperatures for 10 hr in air. All samples annealed at $T \leq 400$°C maintained the hexagonal MoO_3 structure,

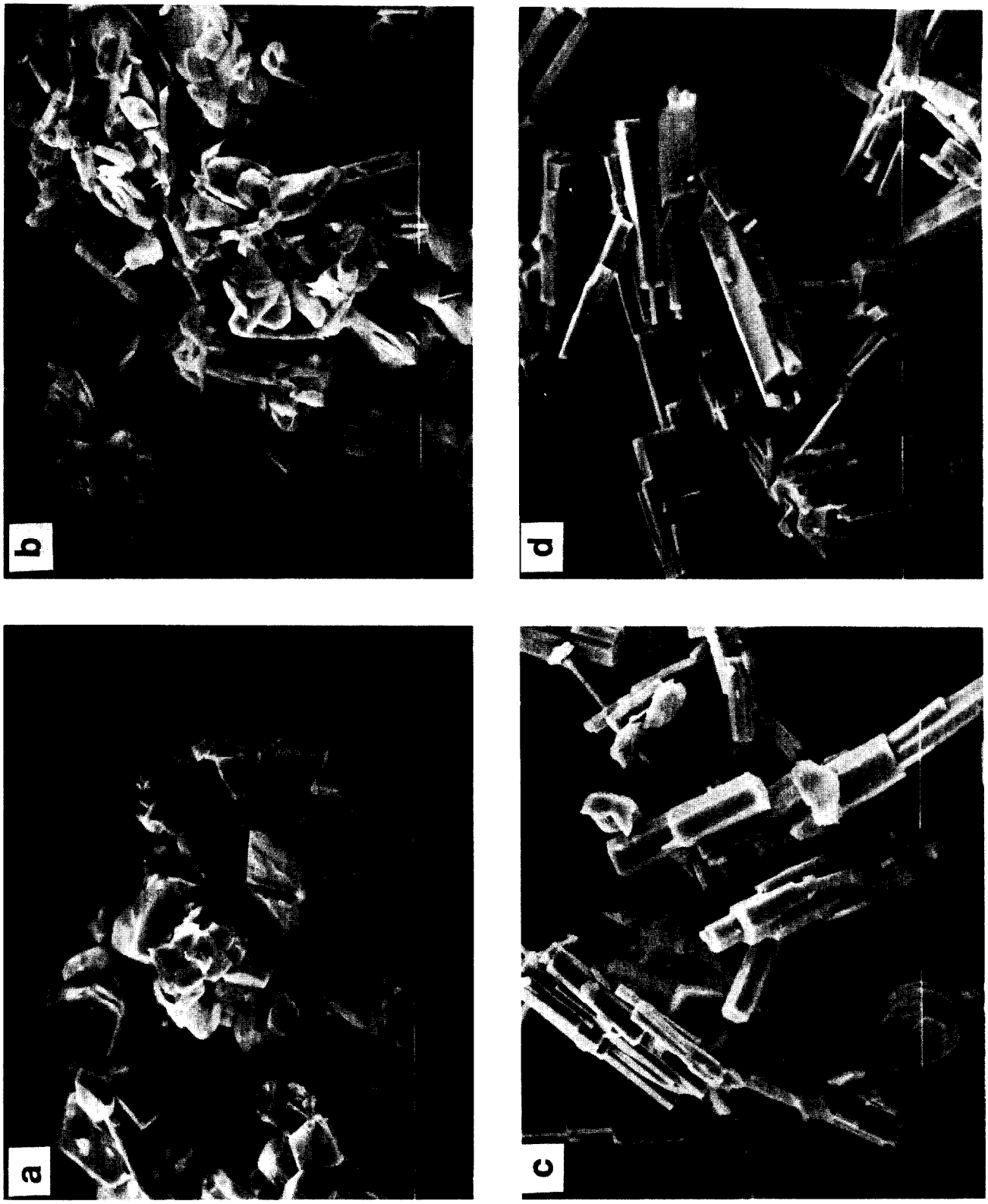

FIG. 3. SEMs collected from samples: (a) before reaction; (b) after 16 hr; (c) after 32 hr; and (d) after 48 hr of reaction. Marker = 10 μm.

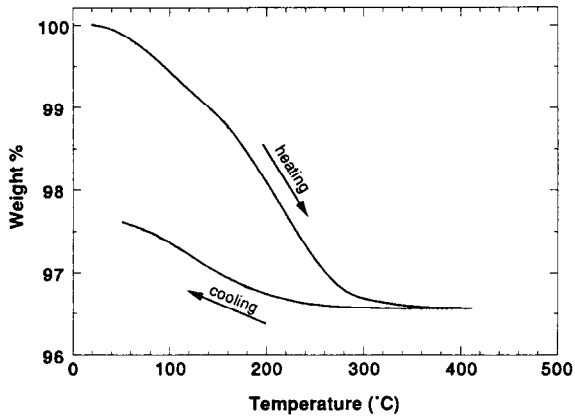

FIG. 4. TGA scans of $Na_{0.13}(V_{0.13}Mo_{0.87})O_3 \cdot nH_2O$ collected on heating and cooling.

while those heated at 410°C showed some degree of bulk decomposition.

3.2. *Solution Synthesis*

In our previous studies of the leaching chemistry of lithium brannerite, we found that the acidic precursor to the open form of the hexagonal MoO_3 structure, $H_{0.13}(V_{0.13}Mo_{0.87})O_3 \cdot nH_2O$, could also be prepared by conventional precipitation methods through the acidification of aqueous Li–V–Mo solutions (4). A similar approach was used to prepare the sodium isomorphs. The preparation of the pure molybdate form of sodium hexagonal MoO_3, $NaMo_{6-x}(\phi_{Mo})_xH_{6x-1}O_{18} \cdot 2H_2O$ ($x \approx 2/3$), from acidic solutions has been reported by McCarron *et al.* (8); given the existence of that compound it seemed likely that a range of compositions could be stabilized with V : Mo contents from 0 : 1 to 0.13 : 0.87. Therefore, a series of Na–V–Mo solutions was prepared with V : Mo concentrations ranging from 0 : 1 to 0.2 : 0.8 and acidified to pH 1.0; see Table 1. This pH was chosen as it was found to yield single-phase hexagonal precipitates in our studies of the Li–V–Mo system (4). Precipitates began to form shortly after the solutions were stirred at 80°C and the reactions were generally complete within 2 hr. The solids collected from the solutions containing vanadium were yellow, while the pure molybdate was white with a blue tint.

Figure 5 shows the powder X-ray diffraction patterns of the precipitates obtained from each of the solutions identified in Table 1. Aside from changes in the relative peak intensities, the patterns are very similar and correspond to a single-phase hexagonal MoO_3 product. The morphologies of the pure molybdate crystallites are strikingly different from those of the vanadium-stabilized phases; the former are quite irregular in shape, while the

TABLE 1
Composition of Solutions and Their Precipitates, $NaV_xMo_{6-x-y}(\phi_M)_yH_{x+6y-1}O_{18} \cdot 2H_2O$

	Sample No.				
	1	2	3	4	5
V% (solution)	0.0	5.0	10.0	15.0	20.0
x	0.0	0.20	0.44	0.65	0.84
y	0.52	0.27	0.16	0.10	0.06
V% (precipitate)	0.0	3.5	7.5	11.0	14.1
ϕ_{Mo} (%)	8.7	4.5	2.7	1.7	1.0

TABLE 2
Refined Atomic Positions, Isotropic Temperature Factors, and Site Occupancies for $Na_{0.13}(V_{0.13}Mo_{0.87})O_3 \cdot nH_2O$ (25°C)

Atom	Site	x	y	z	B(Å^2)	Occup.
Na	6*c*	0.122(8)	0.12(1)	0.17(4)	1.9(9)	0.12(3)
O_w	2*a*	0	0	0.17(2)	8.1(9)	0.24(2)
H	6*c*	0.104(7)	0.006(6)	0.18(2)	2.7(8)	0.01(2)
D						0.15(2)
V	6*c*	0.3549(7)	0.4596(6)	0.72(1)	0.78(9)	0.16(1)
Mo						0.84(1)
O(1)	6*c*	0.2648(6)	0.2757(7)	0.72(1)	1.31(6)	1.00
O(2)	6*c*	0.2174(7)	0.5008(8)	0.698(8)	0.85(8)	1.00
O(3)	6*c*	0.4187(7)	0.4997(7)	0.21(1)	0.61(6)	1.00

Note. Space group: $P6_3$, a = 10.628(1) Å, c = 3.6975(7) Å R_p = 0.080, R_{wp} = 0.106, R_B = 0.061.

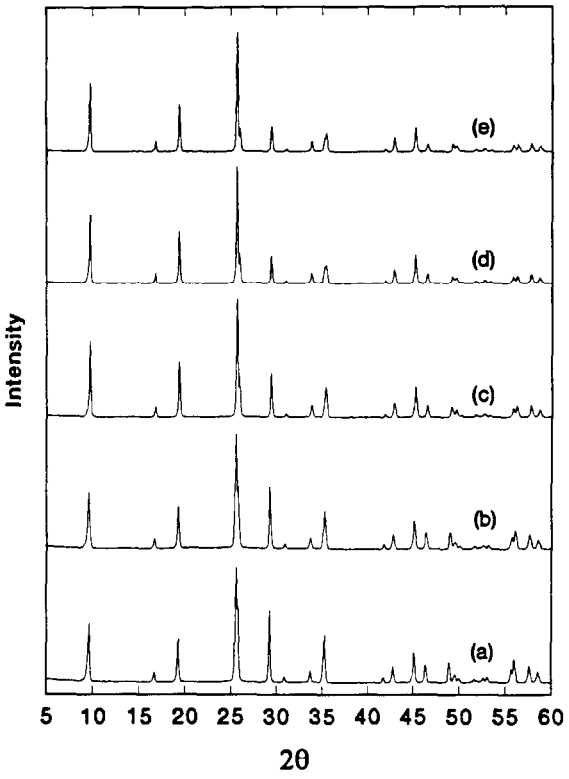

FIG. 5. X-ray diffraction patterns of the solids precipitated from Na=V=Mo solutions at 80°C with pH 1.0, [V + Mo] = 0.15 *M*, and V : Mo = (a) 0 : 1; (b) 0.05 : 0.95; (c) 0.1 : 0.9; (d) 0.15 : 0.85; and (e) 0.2 : 0.8.

latter form perfect hexagonal prisms—see Fig. 6. Solutions containing a higher concentration of vanadium were also studied; however, these yielded two-phase precipitates of the hexagonal phase and a brown amorphous material that we believe to be hydrated V_2O_5. The compositions of hexagonal precipitates were determined from the results of atomic absorption and thermogravimetric analyses. The general formula for these phases can be expressed as $NaV_xMo_{6-x-y}(\phi_M)_yH_{x+6y-1}O_{18} \cdot nH_2O$ ($n \approx 2$) with $0.0 \leq x \leq 0.84$ and $0.0 \leq y \leq 0.52$. The values of x and y for each sample are listed in Table 1. As would be expected, the relative ratio of vanadium to total transition metal content of the precipitates, $x/(6 - y)$, increases linearly with the concentration of vanadium in the aqueous solution and correspondingly the concentration of transition metal vacancies, $y/6$, is reduced. However, it is important to note that the analyses indicate that all the phases formed via the precipitation reactions contain transition metal vacancies in the hexagonal framework, ranging from 8.7% in the pure molybdate to 1.0% in samples with the maximum vanadium content, and one sodium ion per unit cell. This should be contrasted with an apparent absence of vacancies and the correspondingly lower concentration of sodium in the hexagonal phase formed by the acid-leaching of sodium brannerite, whose unit cell formula can be written $Na_{0.78}(V_{0.78}Mo_{5.22})O_{18} \cdot nH_2O$.

The lattice parameters of the precipitates were determined using a Si internal standard and are presented as a function of the vanadium concentration in Fig. 7. The *a* parameter, which to some degree represents the size of the tunnels, is almost constant at 10.64 Å for all the samples, which *c* decreases linearly as the vanadium concentration increases with c (Å) = $(3.727 - 0.166) \times 10^{-2} \times V\%_{(solid)}$. The cell parameters of all the solution precipitates are larger, by amounts that are well outside the limits of experimental error, than those of the vanadium-stabilized samples prepared by acid-leaching.

The precipitation of the sodium hexagonal MoO_3 structures differs from the reactions previously reported for the Li–V–Mo system in three main respects. First, the hexagonal phases in the Na system can be formed with V : Mo framework concentrations ranging from 0 : 1 to 0.14 : 0.86, whereas those in the Li system could be stabilized only with a fixed V : Mo content of 0.13 : 0.87. Second, the hexagonal products in the Na–V–Mo system could be prepared from solutions with a wide range of compositions and also over a broad range of pH values. For example, we found that hexagonal phases were obtained from solutions with a pH as low as 0; in the Li system the successful precipitation of the hexagonal structure occurred in only a narrow range of composition and pH. Finally, although for the Li system the chemistry and thermal stability of the precipitates obtained from the acidic solutions were identical to those produced from the acid-leaching reaction of lithium brannerite, in the sodium system this is not the case. The sodium contents of the solution-derived precipitates are consistently higher than those of the brannerite-derived hexagonal phases and according to the compositional analyses they always contain vacancies in the transition metal framework.

Although the analytically derived concentrations of vacancies are quite low, we found that they have a pronounced effect on the thermal stability of the hexagonal structure. Using the same annealing procedures applied to samples produced by acid-leaching, it was found that the high-temperature stability of $NaV_xMo_{6-x-y}(\phi_M)_yH_{x+6y-1}O_{18} \cdot nH_2O$ increased with increasing concentrations of vanadium. For example, sample 1 decomposed at 310°C and sample 5 at 350°C. The destabilizing effect of the vacancies in the transition metal framework observed in these samples is consistent with the significantly higher thermal stability of brannerite-derived $Na_{0.13}(V_{0.13}Mo_{0.87})O_3 \cdot nH_2O$, which is stable to 400°C and apparently contains no vacancies in the structural framework. The different stabilities are illustrated in Fig. 8, which shows the XRD patterns of the solution- and brannerite-derived sodium hexagonal MoO_3 phases with V : Mo ≈ 0.13 : 0.87

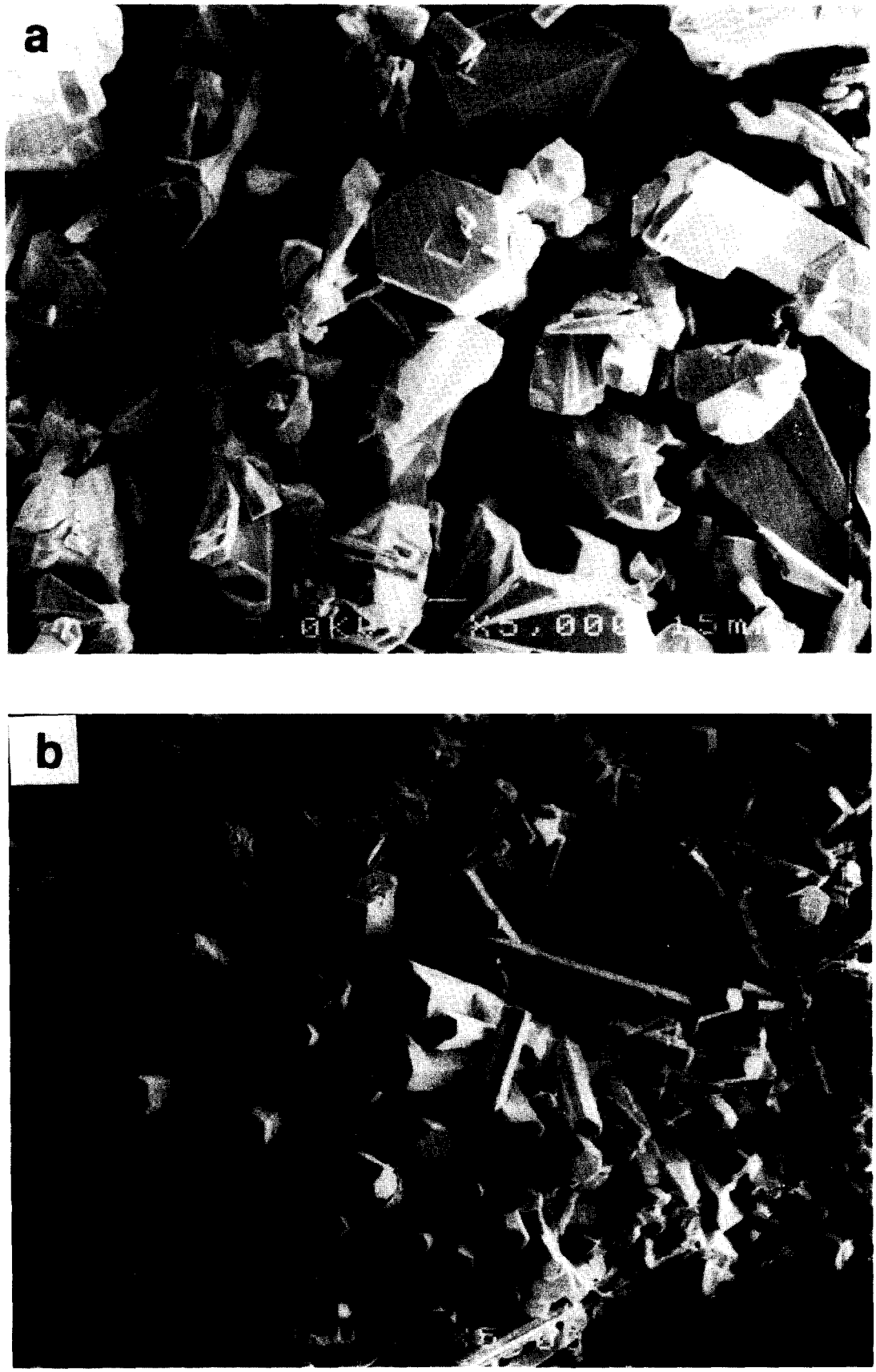

FIG. 6. SEMs of the hexagonal MoO_3 precipitates formed from solutions with pH 1.0 and V : Mo = (a) 0 : 1; (b) 0.2 : 0.8. Marker = 10 μm.

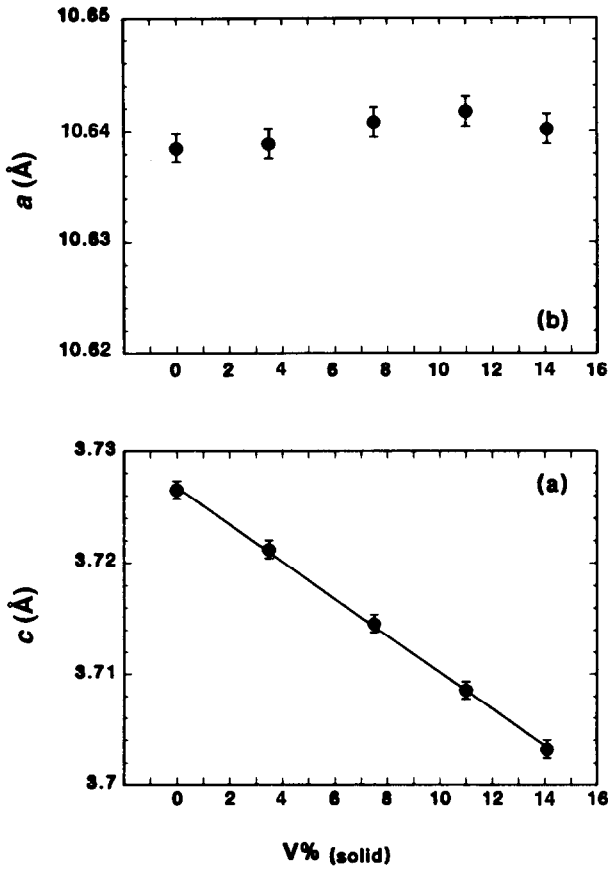

FIG. 7. Variation of a and c as a function of the vanadium content for the hexagonal solution precipitates, $NaV_xMo_{6-x-y}(\phi_M)_yH_{x+6y-1}O_{18} \cdot 2H_2O$.

after annealing at 400°C. These results indicate that although compounds with the hexagonal MoO_3 structure can clearly be prepared via conventional solution precipitation, these methods do not offer an alternative to the preparation of $Na_{0.13}(V_{0.13}Mo_{0.87})O_3 \cdot nH_2O$, which apparently possesses a stoichiometry that is unique to the acid-leaching method of preparation.

Finally it should be noted that the composition of the pure hexagonal sodium molybdate prepared in this work is slightly different from that reported by McCarron *et al.* (8). Expressing the stoichiometry as $NaMo_{6-x}(\phi_{Mo})_xH_{6x-1}O_{18} \cdot 2H_2O$, $x = 0.52$ for the samples prepared in this work while those reported by McCarron *et al.* correspond to $x = 0.67$. This difference does not seem to result from analytical error, as these two samples show different degrees of water loss during thermal decomposition, 5.63% versus 7.8%, and they have quite different lattice parameters, $a = 10.638(1)$ Å and $c = 3.7265(7)$ Å in this work versus $a = 10.595(2)$ Å and $c = 3.722(1)$ Å in McCarron's studies. It is more likely that differences in the details of the sample preparation are responsible for the lower vacancy contents in our compounds. In our precipitation reactions the solution was only moderately acidified ($H^+/MoO_4^{2-} \approx 3.5$, where H^+ is the total amount of H^+ added), while in McCarron *et al.*'s preparation the acidity was much higher ($H^+/MoO_4^{2-} \approx 7$); the concentration of sodium in our solutions, [Na] : [V + Mo] = 3 : 1, was also slightly higher than those used in the previous preparations in which [Na] : [V + Mo] was 2 : 1. It is reasonable to assume that the exact value of x depends on the composition and the degree of acidification of the solution.

3.3. *Structure Refinement of* $Na_{0.13}(V_{0.13}Mo_{0.87})O_3 \cdot nH_2O$

Deuterated samples of $Na_{0.13}(V_{0.13}Mo_{0.87})O_3 \cdot nH_2O$ were prepared by exchanging the acid-leaching products of sodium brannerite in D_2O and examined using neutron diffraction. Vibration bands from both O–H (≈3550, 1620 cm^{-1}) and O–D (2610, 1210 cm^{-1}) were observed in the FTIR spectra of these samples, indicating that the hydrogen atoms were not completely exchanged by deuterium. The apparent systematic absences (001, $l = 2n + 1$) observed in the powder X-ray patterns were consistent with

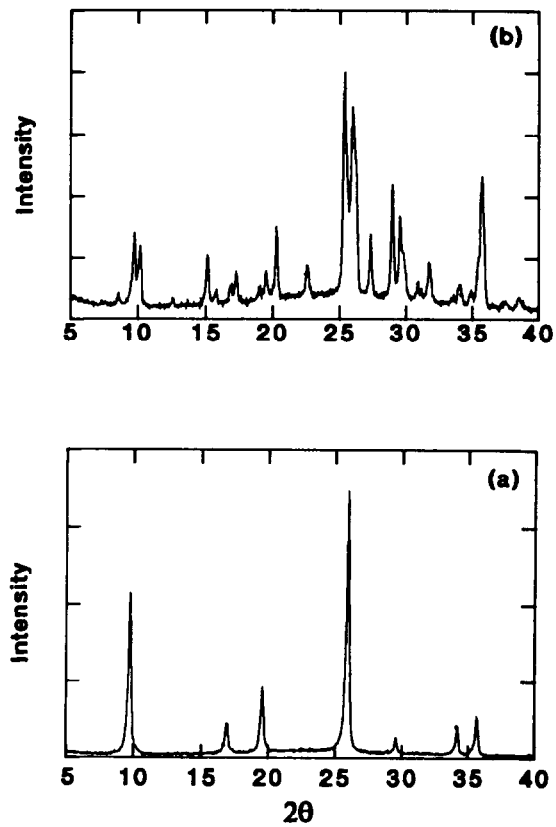

FIG. 8. Powder X-ray diffraction patterns of sodium hexagonal MoO_3 phases after annealing at 400°C, (a) prepared via leaching of sodium brannerite and (b) prepared by precipitation from Na–V–Mo solution with V : Mo = 0.2 : 0.8.

space groups $P6_3$ and $P6_3/m$. Although the modeling of the neutron data was attempted using both space groups, $P6_3$ gave lower R values and was ultimately chosen for the final structure refinement using a cell with $a = 10.628(1)$ Å and $c = 3.6975(7)$ Å. During the refinement pseudo-Voigt peak profile and polynomial background functions were used and the following parameters were refined: zero-point, background parameters, scale factors, lattice parameters, FWHM parameters, peak profile parameters, peak asymmetry parameter, preferred orientation parameters, atomic positions, isotropic temperature factors, and site occupancies. No anisotropic temperature factor refinement was attempted. The 2θ regions containing Bragg reflections from the aluminum sample container were excluded from the refinement.

Because the structure of the hexagonal MoO_3 framework has been well studied and the contribution from Na and $(D,H)_2O$ to the total diffraction intensity was relatively low, a combination of Rietveld refinement and difference Fourier synthesis was used to solve the structure of $Na_{0.13}(V_{0.13}Mo_{0.87})O_3 \cdot nH_2O$. By starting with the atomic coordinates and temperature factors of the framework ions in the open hexagonal structure, $(V_{0.13}Mo_{0.87})O_{2.935}$ (4), the structure refined to $R_p = 0.112$, $R_{wp} = 0.162$, and $R_B = 0.121$. To locate the positions of the Na, (D, H), and O atoms in the channels two-dimensional difference Fourier maps were constructed in $0.1z$ increments along c. The difference Fourier maps contained two maxima inside the channel on the same a–b plane at $z = 0.2$. The peak with the higher intensity was located in the center of the channel at (0, 0, 0.2), while the weaker peak was located off the center of the channel toward the perimeter of the framework at (0.10, 0.01, 0.2). These two peaks were separated by approximately 1 Å. Based on geometrical considerations, the first peak was assigned to oxygen (O_w) and the second to deuterium. By including these atoms in the refinement, the R values dropped significantly to $R_p = 0.082$, $R_{wp} = 0.108$, and $R_B = 0.062$, with an oxygen occupancy of 0.25 at (0, 0, 0.18), a deuterium occupancy of 0.14 at (0.103, 0.005, 0.18), and a D–O_w bond length of 1.07 Å. Because the diffraction data were actually collected on partially rather than completely deuterated samples, the occupancy of this position is actually due to a combination of D and H. Without a fixed constraint for the sum of the occupancies, it was not possible to refine D and H occupancies independently. To solve this problem the concentration of (D, H) was constrained to be twice that of O_w and the real occupancy of H and D was calculated from the pseudo-occupancy of a pure D atom using

$$b_D x_D + b_H x_H = b_D x_{pseudo} \quad [1]$$

$$x_D + x_H = 2x_{Ow}/3, \quad [2]$$

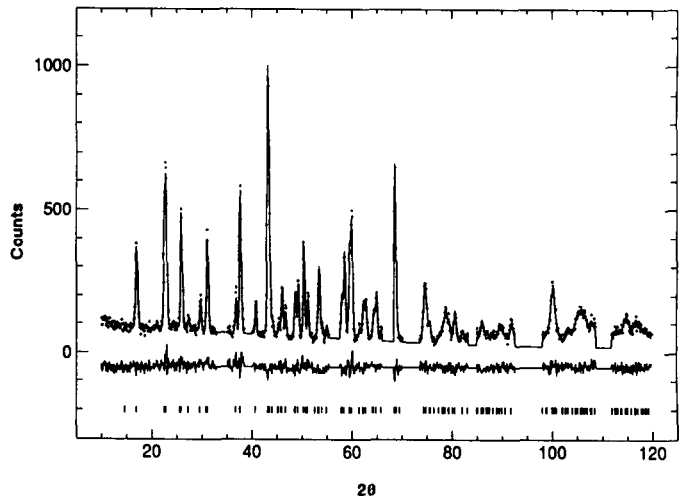

FIG. 9. Observed (dot), calculated (solid line) powder neutron diffraction patterns of $Na_{0.13}(V_{0.13}Mo_{0.87})O_3 \cdot nH_2O$, and their difference. Bars indicate positions of Bragg reflections.

where x_D, x_H, and x_{pseudo} are the H, D, and pseudo-occupancies, and b_D and b_H are the diffraction cross sections for D and H. The results from the final refinement indicated that the actual concentration of H was quite small; see Table 2.

To locate the missing sodium atoms, two-dimensional difference Fourier maps were again constructed along the c axis. Several diffuse peaks with fairly weak intensities were observed. Although most of these peaks were in positions that would yield unrealistic bond lengths, one peak at (0.13, 0.12, 0.2) corresponded to a reasonable location for the sodium ions in the channels. This sodium atom was included in the final refinement for which the agreement indices were $R_p = 0.080$, $R_{wp} = 0.106$, and $R_B = 0.061$. The final results for the refined atomic positions, occupancies, and isotropic thermal factors are listed in Table 2. The low value for the sodium occupancy, which is in excellent agreement with that obtained through the chemical analyses, is consistent with the weak intensities found in the Fourier difference maps. Selected interatomic distances for the final structure are presented in Table 3 and Fig. 9 shows the observed and calculated neutron patterns together with their difference.

Based on the refinement results, the water molecules reside in the channels of the structure with the O_w atom being positioned in the center of the channel ($2a$ site). In one unit cell there are two equivalent positions for the O_w atoms in each channel. The close proximity of these sites, which are separated by 1.85 Å = $c/2$, precludes their simultaneous occupation and necessitates an O_w occupancy of less than 0.5. The refined O_w occupancy in the structure is 0.24, which satisfies this criterion. The D(H) atoms associated with the water molecules are lo-

TABLE 3
Interatomic Distances (Å) in $Na_{0.13}(V_{0.13}Mo_{0.87})O_3 \cdot nH_2O$

MO_6 octahedra		NaO_6 octahedra			
M–O(1)	1.69	Na–O(1)	2.30	O_w–Na	2.25
M–O(2)	1.72		2.44	O_w–D	1.07
	2.37		2.56	O_w–O(1)	2.88
M–O(3)	1.91		2.58		
	1.98	Na–O_w	2.25	D–O(1)	1.80
	2.22		2.25	D–O_w	1.07

Note. *M* = Mo or V.

cated in sites that are almost colinear between the O_w and O(1) atom positions. The O_w–O(1) distance is 2.87 Å, which is consistent with hydrogen bonding of intermediate strength between the water molecules and terminal oxygen atoms (14–17). The O_w–D and D · · · O(1) interatomic distances are 1.07 and 1.80 Å, respectively; the former is at the upper end of the bond lengths typically observed for an O–H bond and is consistent with those usually found in disordered structures with partial occupancies, for example, KH_2PO_4 (18), $H_{0.34}MoO_3$ (19), and $H_{0.52}WO_3$ (20).

The Na atoms in the structure are located in positions between the center of the channels and the perimeter of the vanadate–molybdate framework. Although the refined positions of Na and O_w are almost on the same *a*–*b* plane, based on geometric considerations the actual positions of the sodium cations in the structure must be shifted by *c*/2 along the *c* axis with respect to O_w. This configuration results in an octahedral coordination of Na by oxygen, with four of the nearest neighbor anions coming from the framework (O1) and two from the water molecules (O_w). The resultant Na–O bond lengths are 2.25 (×2), 2.30, 2.44, 2.56, and 2.58 Å. The accuracy of the bond lengths is undoubtedly affected by the thermal motions and in particular by the small occupancies of the Na and O_w positions. Although the Na–O_w bond lengths of 2.25 Å are somewhat short they are not without precedent; for example, similar distances have been reported for hexagonal $Na_{0.24}WO_{3.12} \cdot 0.5H_2O$ (21), $Na_4V_2O_7 \cdot H_2O$ (22), and $Na_{1.8}Be_{0.9}Si_{1.1}O_4$ (23). Even though there are six crystallographically equivalent positions for Na in each unit cell, to avoid unrealistically short Na–Na distances no more than two can be occupied simultaneously. In fact because of the low concentration of sodium in the structure (the refined occupancy is only 0.12) it is not necessary for more than one site to be occupied in each unit cell. In Fig. 10 the NaO_6 octahedra in $Na_{0.13}(V_{0.13}Mo_{0.87})O_3 \cdot nH_2O$ have been drawn to illustrate a random occupation for each unit cell.

As one might expect, the sodium positions in this structure are similar to those reported for $NaMo_{5.33}(\phi_{Mo})_{0.67}H_3O_{18} \cdot 2H_2O$ by McCarron *et al.* (8). However, the degree of hydration reported for the pure molybdate is significantly higher than the occupancy we have found in the vanadium-stabilized sodium molybdate. Because a water content greater than one molecule per unit cell would result in O–O bond lengths of 1.85 Å, it is possible that some of the additional water in their structure is associated with the surface rather than the bulk. It is clear that the water molecules play a critical role in stabilizing the

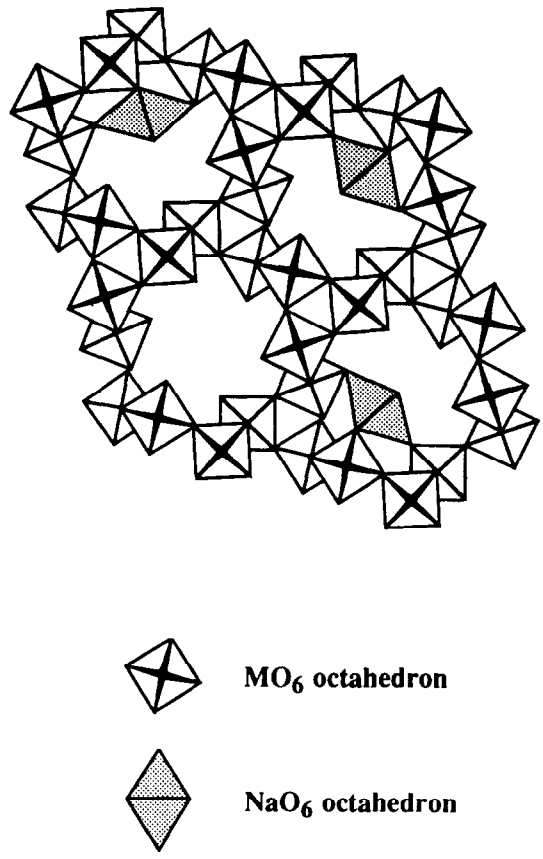

FIG. 10. Schematic illustration of the structure of $Na_{0.13}(V_{0.13}Mo_{0.87})O_3 \cdot nH_2O$; sodium octahedra are shown for random occupation in the unit cell.

sodium form of the hexagonal MoO_3 structure. Without these additional ligands located above and below, the Na cations would be unable to adopt any suitable coordination environments. It is probably for this reason that the sodium isomorph has been synthesized only in an aqueous medium and not by solid-state reaction. However, once prepared, the structure does apparently have some limited region of stability in the dehydrated form, though perhaps kinetic rather than thermodynamic, and decomposes approximately 100°C above the temperature at which it loses the structural water.

The water content obtained for $Na_{0.13}(V_{0.13}Mo_{0.87})O_3 \cdot nH_2O$ from the refinement ($n = 0.083$) is about one-third the value determined from the thermogravimetric analyses where $n \approx 0.26$. It is likely that the difference in these two determinations is due to water adsorbed on the surface of the hexagonal MoO_3 crystallites. This argument is supported by the weight gain observed upon cooling, which corresponds to the rehydration of approximately 0.09 mole of H_2O, which is in close agreement with the values obtained from the neutron refinement. It should be noted that the surface desorption continues to temperatures close to 200°C, indicating that these groups are quite strongly bonded. Similar effects have been reported for $WO_3 \cdot nH_2O$ ($n \approx 0.5$) (24) and $Na_{0.24}WO_{3.12} \cdot 0.5H_2O$ (21), where different water contents were obtained via the thermogravimetric and structural analyses and desorption also continued to relatively high temperatures. Gerand *et al.* (24) have suggested that the adsorbed water in these systems is present in a molecular form and as surface –OH groups; it is these rather strongly bonded –OH groups that are responsible for the relatively high temperature for desorption. Because of the Mo=O terminal groups that are present in the structure of hexagonal MoO_3, it is likely that some of the adsorbed water in $Na_{0.13}(V_{0.13}Mo_{0.87})O_3 \cdot nH_2O$ is also bonded in the form of OH groups. Some support for this hypothesis comes from IR studies in which the presence of adsorbed water hydrogen bonded to adsorbed OH groups was confirmed by the observation of broad bands at 1630 and 3500 cm^{-1}.

4. DISCUSSION

Although the products obtained from the leaching reaction of sodium brannerite and by direct precipitation from acidified Na–V–Mo solutions all have the hexagonal MoO_3 structure, their stoichiometries are not the same. In particular it has been shown that the solution-derived phases, $Na_{0.167}V_xMo_{1-x-y}(\phi_M)_yH_{x+6y-0.167}O_3 \cdot nH_2O$ ($x \leq 14$, $y \leq 0.09$, $n \approx 0.33$), contain a higher concentration of sodium, one per unit cell, which is charge compensated by vacancies in the transition metal framework. These compositional and structural differences result in a lower thermal stability for the solution-derived hexagonal molybdates than for their brannerite-derived counterparts. The unique stoichiometry and stability of the acid-leaching product may imply that this reaction does not proceed via a simple dissolution/reprecipitation mechanism and that it is somehow facilitated by a structural relationship between the brannerite solute and the hexagonal precipitate. To gain some further insight into the path of this reaction additional solution precipitation experiments were conducted under conditions that mimicked those present during the leaching of sodium brannerite.

During the leaching reaction of sodium brannerite solid phases are present during the entire course of the transformation to hexagonal MoO_3, which begins to form after approximately 5 hr. For the reaction of 1 g of $NaVMoO_6$ in 50 ml of HCl, 0.28 g (≈0.001 mole) of the solute dissolves into solution, which was found to have pH 0.70, before the initial appearance of the hexagonal phase. These conditions were duplicated by preparing an aqueous Na–V–Mo solution with the same composition and pH from other solutes. This was accomplished by first dissolving 0.122 g of $NaVO_3$ (0.001 mole) in 10 ml of water to produce an Na–V solution. This solution was then mixed with a separate solution of 0.206 g of Na_2MoO_4 (0.001 mole) in 15 ml of water which had been repeatedly passed through an ion-exchange column to remove all the Na. After addition of 2.0 *M* HCl and water to adjust the volume and pH to 50 ml and 0.70, respectively, the solution was stirred at 60°C. While the sodium brannerite reaction produces the hexagonal phase after 5 hr, no precipitation was observed from the duplicate solutions even after 1 week. This result lends further support to the idea that the crystal chemistry of the brannerite "solute" plays a significant role in the formation of the hexagonal molybdate structure via the leaching reaction route. Before further discussion of the brannerite reaction, it is useful to review the other examples of this type of leaching chemistry that have appeared in the literature.

Leaching reactions, in which a solid reacts with a percolating solution to dissolve a reactive fraction, are originally associated with the selective removal of solid phases from a compositionally heterogeneous mixture. Although this type of reaction is well known and widely used, for example, in mineral extraction technology, the leaching chemistry (or acid digestion) of compositionally and structurally homogeneous phases is not as well recognized and has been reported for only a few selected solids. In several of these examples this type of soft chemistry has resulted in the formation of new metastable compounds such as λ-MnO_2 (25), fluorite-type $LnCl_2$ (*Ln* = Eu, Sm), and anti-Fe_2P-type BaX_2 (*X* = Cl, Br) (26).

All of the homogeneous solids that participate in an acid-leaching reaction contain at least two ions with different bulk solubilities and can be grouped into the following two categories: (1) mixed-valence compounds, in which

TABLE 4
Examples of Acid-Leaching Reactions

"Solute"	Product/stability	Soluble species	Structural "filiation"	Ref.
Pb_3O_4	PbO_2 (stable)	Pb^{2+}	Columns	(30)
Ti_3O_5	TiO_2(II) (metastable)	Ti^{3+}	Layers	(29)
$LiMn_2O_4$	λ-MnO_2 (metastable)	Mn^{2+}	Framework	(25)
Li_2MnO_3	$Li_{0.36}Mn_{0.91}O_2$ (metastable)	Li	Fragment	(31)
$NaVMoO_6$	$Na_{0.13}(V_{0.13}Mo_{0.87})O_3$ (hex. MoO_3; metastable)	V^{5+}	Fragment	This work
$Ln_{14}Cl_{33}$ (Ln = Eu, Sm)	$LnCl_2$ (fluorite, metastable)	Ln^{3+}	Layers	(26)
$Ba_9Ln^5Br_{33}$ (Ln = La, Nd)	$BaBr_2$ (anti-Fe_2P, metastable)	Ln^{3+}	Layers	(27)

the same metallic element is present in two different oxidation states, for example, $Tb_{11}O_{20}$ (27), Pr_7O_{12} (28), Ti_3O_5 (29), and Pb_3O_4 (30), and (ii) compounds with two different metallic elements, for example, Li_2MnO_3 (31) and $NaVMoO_6$ studied in this work. The acid-leaching of $LiMn_2O_4$ to form λ-MnO_2 involves a combination of both types of reaction (25).

In each documented example of this type of reaction the structure of the product bears a strong structural filiation to that of the reactant; see Table 4. The structural similarities range from the entire framework, e.g., $LiMn_2O_4$, to two-dimensional sheets, e.g., Ti_3O_5, to one-dimensional chains, e.g., Pb_3O_4, to isolated clusters or fragments, e.g., Li_2MnO_3. Given these simlarities, for some compounds it has been suggested that the leaching reaction involves a topotactic solid-state ransformation in which significant parts of the solute structure are retained during the leaching process. The conversion of the spinel $LiMn_2O_4$ to a metastable, defect spinel form of λ-MnO_2 is an example where the entire framework is preserved during the leaching process. In the mechanism proposed by Hunter (25) the Mn^{3+} ions at the surface of $LiMn_2O_4$ disproportionate to Mn^{4+} and Mn^{2+} and the soluble Mn^{2+} and Li^+ ions at the surface are leached into the acidic solution. The diffusion of Li^+ from the interior of the crystallites to the surface and electron-hopping from the surface to the interior supply additional species for further dissolution and provide a mechanism for the conversion of $LiMn_2O_4$ to λ-MnO_2 without any bulk structural rearrangement. The leaching reactions of $Tb_{11}O_{20}$ to TbO_2 and Pr_7O_{12} to PrO_2 have been reported to proceed through a similar route (27, 28). In both cases the more soluble trivalent rare-earth ions are dissolved from selective reaction pits, usually intersections of dislocations and the surface, to yield Tb^{3+}(aq)/Pr^{3+}(aq). The dissolution is accompanied by oxygen transport from the reaction pits into remote regions where $Tb_{11}O_{20}/Pr_7O_{12}$ are topotactically oxidized to TbO_2/PrO_2. Because the entire topology of the solute structure is preserved in these examples, alternative methods can be used to synthesize the same metastable product. For example, λ-MnO_2 can be prepared electrochemically by deintercalating Li from $LiMn_2O_4$. However, when only certain structural units or fragments of the leachant phase are preserved, acid-leaching seems to provide a unique route to the metastable product. For example, Grey *et al.* have reported on the ambient pressure conversion of Ti_3O_5 to a metastable, high-pressure form of TiO_2 with the α-PbO_2 structure, TiO_2(II), by leaching in H_2SO_4 (29). In this case the arrangement of the Ti ions in certain planes of α-Ti_3O_5 are essentially identical to those in the TiO_2(II) product. Again it was suggested that these crystallographic features of the solute are preserved during the leaching reaction. The transformations of mixed valence halides to fluorite-type $LnCl_2$ for Ln = Eu and Sm and the formation of anti-Fe_2P-type BaX_2 (X = Cl, Br) from barium-rare earth halides (26) are further examples of leaching reactions in which layers of the reactant are preserved and are claimed to proceed via a solid-state transformation mechanism.

However, some of the other examples of acid-leaching reactions have been interpreted in terms of a more conventional dissolution/recrystallization mechanism. For example, in their studies of the acid-leaching of Pb_3O_4 to PbO_2, Kang *et al.* (30) demonstrated that this reaction proceeds via the bulk dissolution of Pb_3O_4 at the surface and the reprecipitation of the less soluble Pb^{4+} ions as PbO_2. In contrast to the metastable products formed via the solid-state transformation mecha-

nism, this reaction produces a thermodynamically stable, rutile form of PbO_2.

For the acid-leaching reactions involving a solid-state transformation mechanism the crystallography of the reactant is crucial, while for those proceeding via a dissolution/recrystallization mechanism, it is possible that the structure of the reactant is unimportant. The results we have obtained in this work for the acid-leaching of sodium brannerite would suggest that this system falls into the former category and that the structure of the brannerite solute affects the mechanism of formation and the composition of the hexagonal MoO_3 structure. To ascertain the exact role of the solute structure it would be necessary to conduct detailed studies of the solid–solution interface and of the solution species that are formed during the partial dissolution of brannerite. Some attempts were made to identify the solution species using ^{51}V NMR; however, these experiments were not fruitful as the peaks were extremely broad.

Even without this type of detailed information it is possible to speculate on which aspects of the precipitation reaction are influenced by the crystallography of the solute. Perhaps the most obvious mechanism for the influence of the brannerite structure would be for it to act as a substrate for the oriented nucleation and growth of the hexagonal molybdate phase. If this was the case, it would be expected that in the resultant precipitate many of the grains would contain coherent interfaces between the "solute" and "precipitate." In fact this was never observed and all the precipitates collected at various stages of the reaction were composed of discrete particles of the hexagonal MoO_3 and brannerite phases.

The solution with the same composition and pH as those formed during the initial stage of the leaching reaction of sodium brannerite did not produce the hexagonal MoO_3 phase. This suggests that the formation of the solution species which serve as the "building blocks" for the hexagonal structure is facilitated by the presence of the brannerite solute. Therefore, instead of providing a mechanism for oriented nucleation and growth, it is possible that the slow dissolution of the brannerite structure may be critical in providing a unique rate of formation and concentration of the solution precursors to the hexagonal phase. Furthermore, the possibility that these brannerite-derived solution species may have a unique structure and composition cannot be discounted. Before further discussion on the mechanism it is useful to reconsider the structural similarities of brannerite and hexagonal MoO_3. Although from the projections presented in Fig. 1, [010] for brannerite and [001] for hexagonal MoO_3, these two structures look quite different, by projecting along [001] for brannerite and [010] for hexagonal MoO_3 it is clear that there is a strong filiation between these two crystal structures; see Fig. 11. Both structures are constructed

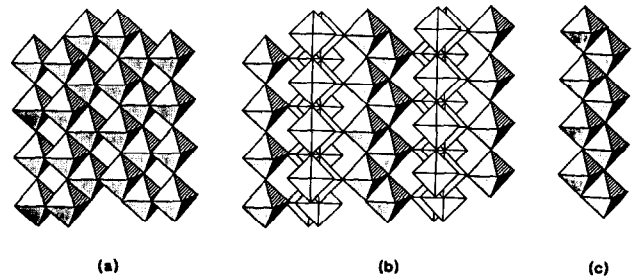

FIG. 11. Structure projections of (a) brannerite along [001], (b) hexagonal MoO_3 along [010], and (c) their common structural unit.

from the same infinite zigzag chain of edge-sharing (V, Mo)O_6 octahedra; in brannerite these chains share edges, whereas in hexagonal MoO_3 they are linked by corner-sharing.

As discussed in Section 3, our studies using SEM and XRD showed that during the acid-leaching reaction there is a preferential dissolution of the Na brannerite structure along the [001] direction, which is perpendicular to the zigzag brannerite layers. This would imply that during the dissolution the acid "attacks" the solid by removing individual layers of the structure. Because the zigzag chains of edge-sharing octahedra are contained within the brannerite layers, it is possible that although the dissolution process destroys the overall integrity of the brannerite structure, extended fragments of the zigzag chains are preserved. It is then conceivable that these solvated chain fragments can recombine to form the hexagonal MoO_3 structure.

While the leaching reaction of $NaVMoO_6$ yields a hexagonal MoO_3 framework that contains no transition metal vacancies, the phases obtained via the direct solution method always contain framework vacancies that are charge balanced by a higher concentration of sodium in the channels of the structure. These differences may result from the formation of the extended chain fragments postulated above and/or they could arise from differences in the rate of formation of the solution precursors in the two methods. In the leaching reaction the low solubility and slow dissolution of $NaVMoO_6$ in dilute acid may provide a constant, low-concentration source of the solvated building blocks of the hexagonal MoO_3 structure and ensure a slow growth of a vacancy-free precipitate. In the direct solution precipitation method the high concentration of V and Mo may result in a high concentration of the solution precursors to the hexagonal structure and a rapid precipitation, which was typically completed within 2 hr. This high growth rate may in turn be partially responsible for the formation of a defect framework that contains transition metal vacancies.

In summary, the similarity between Na brannerite and hexagonal MoO_3 structures appears to promote the forma-

tion of a low concentration of the requisite solvated precursors that serve as a template for the precipitation reaction. In these dilute molybdo-vanadate solutions the absence of a brannerite solute apparently completely suppresses or significantly reduces the rate of formation of the desired solution species. It is proposed that the constant supply of a low concentration of solution species results in the slow growth of a defect-free hexagonal MoO_3 phase. Therefore the mechanism of the leaching reaction of Na brannerite is perhaps best described in terms of a combination of a solid-state and dissolution/recrystallization transformation. While the structure of the solute apparently influences the concentration and stability of the solvated polyanions, their formation, condensation, and reprecipitation in the hexagonal MoO_3 structure proceed via solution and are spatially separated from the source of the dissolution reaction.

We conclude by drawing attention to acid-leaching as an effective method for the soft chemical synthesis of new metastable materials. Several examples have already been documented in the literature and some of these, e.g., λ-MnO_2, have proven to have important technological applications. It seems unlikely that those systems and the compounds examined in this work are the only examples of this phenomenon. To date most of the discoveries of oxides and halides that yield metastable products by acid-leaching have been serendipitous, and no deliberate and systematic attempt has been made to explore the viability of this technique in the synthesis of new metastable materials. Although the search for new examples will still need to rely largely on trial and error, certain guidelines do exist. In all the current examples the "solute" structure contains at least two ions with different bulk solubilities in the leaching medium, and in most cases the materials that participate in this type of reaction lie on a borderline between complete and partial solubility. It would therefore be interesting to explore the solvolytic behavior of several groups of structures that fall into this category. Given the reports of leaching in Li–Mn oxides with rock-salt and spinel structures, related structures that contain different transition metal ions may serve as a useful starting point for this type of investigation.

5. CONCLUSIONS

The hexagonal products of the acid-leaching reaction of sodium brannerite $NaVMoO_6$ have a unique composition and thermal stability that cannot be duplicated in preparations via conventional solution precipitation methods. In all cases the solution-derived hexagonal precipitates contained a higher concentration of sodium within the one-dimensional channels of the structure and cation vacancies in the transition metal framework. Crystallographic similarities between the brannerite and hexagonal MoO_3 structures apparently promote the formation of a low concentration of the requisite solvated precursors that serve as a template for the precipitation reaction. It is proposed that this type of leaching chemistry may provide a unique route for the preparation of several other metastable materials.

ACKNOWLEDGMENTS

This work was supported by the National Science Foundation (Ceramics/Solid State Chemistry Divisions) Grant DMR 94-21184 and through the NSF/MRL program under Grant DMR 91-20668. We also acknowledge the NSF/MRL support for the electron microscopy central facilities.

REFERENCES

1. T. P. Feist and P. K. Davies, *in* "Chemistry of Electronic Ceramic Materials" (P. K. Davies and R. S. Roth, Eds.), SP 804, p. 163. National Institute of Standards and Technology, Gaithersburg, MD (1991).
2. T. P. Feist and P. K. Davies, *Chem. Mater.* **3,** 1011 (1991).
3. Y. Hu, P. K. Davies, and T. P. Feist, *Solid State Ionics* **53/56, 539 (1992).**
4. Y. Hu and P. K. Davies, *J. Solid State Chem.* **105,** 489 (1993).
5. J. Galy and B. Darriet, *C. R. Seances Acad. Sci. Ser. C.* **264,** 1477 (1967).
6. R. Ruh and A. D. Wadsley, *Acta Crystallogr.* **21,** 974 (1966).
7. P. K. Davies and C. M. Kagan, *Solid State Ionics* **53/56,** 546 (1992).
8. E. M. McCarron III, D. M. Thomas, and J. C. Calabrese, *Inorg. Chem.* **26,** 371 (1987).
9. B. Krebs and I. Paulat-Boschen, *Acta Crystallogr. Sect. B* **32,** 1697 (1976).
10. N. A. Caiger, S. Crouch-Baker, P. G. Dickens, and S. G. James, *J. Solid State Chem.* **67,** 369 (1987).
11. J. Guo, P. Zavalij, and M. S. Whittingham, *Eur. J. Solid State Inorg. Chem.* **31,** 833 (1994).
12. B. Darriet and J. Galy, *J. Solid State Chem.* **8,** 189 (1973).
13. I. P. Olenkova, L. M. Plyasova, and S. D. Kirik, *React. Kinet. Catal. Lett.* **16,** 81 (1981).
14. G. C. Pimentel and A. L. McClellan, "The Hydrogen Bond." Freeman, San Francisco/London, 1960.
15. W. C. Hamilton and J. A. Ibers, "Hydrogen Bonding in Solids." Benjamin–Cummins, Redwood City, CA, 1968.
16. G. Ferraris and M. Franchini-Angela, *Acta Crystallogr. Sect. B* **28,** 3572 (1972).
17. G. Chiari and G. Ferraris, *Acta Crystallogr. Sect. B* **38,** 2331 (1982).
18. H. A. Levy, S. W. Peterson, and S. H. Simonsen, *Phys. Rev.* **93,** 1120 (1954).
19. P. G. Dickens and J. J. Birtill, *J. Solid State Chem.* **28,** 185 (1979).
20. P. J. Wiseman and P. G. Dickens, *J. Solid State Chem.* **6,** 374 (1973).
21. K. P. Reis, E. Prince, and M. S. Whittingham, *Chem. Mater.* **4,** 307 (1992).
22. V. Katsuo and E. Takayama-Muromachi, *Acta Crystallogr. Sect. C* **43,** 1025 (1987).
23. S. Frostang, J. Grins, and M. Nygren, *Solid State Ionics* **44,** 51 (1990).

24. B. Gerand, G. Nowogrocki, and M. Figlarz, *J. Solid State Chem.* **38,** 312 (1981).
25. J. C. Hunter, *J. Solid State Chem.* **39,** 142 (1981).
26. G. Liu and H. Eick, *J. Solid State Chem.* **95,** 99 (1991).
27. Z. C. Kang and L. Eyring, *J. Solid State Chem.* **75,** 60 (1988).
28. Z. C. Kang and L. Eyring, *J. Solid State Chem.* **75,** 52 (1988).
29. L. E. Grey, C. Li, and I. C. Madsen, *Mater. Res. Bull.* **23,** 743 (1988).
30. Z. C. Kang, L. Machesky, H. A. Eick, and L. Eyring, *J. Solid State Chem.* **75,** 73 (1988).
31. M. M. Thackeray, *J. Solid State Chem.* **104,** 464 (1993).